

Exploring the Dynamics of Simple Inhibition Systems in Continuous Stirred-Tank Reactor: Mathematical Modelling and Bifurcation Analysis

'Afifi Md Desa^{a,b,*}, Mohd Hafiz Mohd^a, Mohamad Hekarl Uzir^c

^aSchool of Mathematical Sciences, Universiti Sains Malaysia, 11800 USM Penang, Malaysia; ^bInstitute of Engineering Mathematics, Universiti Malaysia Perlis, 02600 Arau, Perlis, Malaysia; ^cSchool of Mathematical Sciences, Universiti Sains Malaysia, 11800 USM Penang, Malaysia

Abstract The simple enzyme inhibition systems consist of competitive inhibition, noncompetitive inhibition and uncompetitive inhibition. In this work, we incorporated these simple inhibition systems in the continuous stirred-tank reactor (CSTR) and analysed the models using some techniques from dynamical systems and bifurcation analysis. Our aim is to investigate the behaviours of such systems and compare their overall dynamics. The phase portrait is constructed to simulate possible behaviours such as stable steady states, stable limit cycle, bistability between the steady state and the stable limit cycle and bistability between two steady states. The systems undergo bifurcational changes in dynamics as enzyme concentration, dilution rate and proportional control constant are varied. Moreover, we conducted a codimension two bifurcation analysis to examine the joint effects of dilution rate and proportional control constant on the systems behaviours. Our results revealed distinct dynamics for each inhibition system. Increasing the dilution rate led to a transition from low to high substrate concentrations, with competitive inhibition showing the highest tipping (or bifurcation) point where dynamical regimes change due to intense substrate-inhibitor competition. Elevating enzyme concentration reduced substrate concentration, particularly in non-competitive inhibition systems due to higher conversion rates. Furthermore, the proportional control constant had varying effects depending on the specific inhibition system. These findings emphasize the on the combined influences of distinct chemical processes in controlling reactor heat and optimizing bioprocess efficiency, considering the unique characteristics of each inhibition system. Overall, the dynamical study on these simple inhibition systems enables us to improve our understanding on the chemical processes involving enzymes with multiple types of inhibitors and may give some insights in its controlling process.

Keywords: Enzyme inhibitions, dynamical systems, bifurcation, phase plane analysis.

Introduction

An inhibitor is defined as a substance that has a tendency to reduce the rate of a reaction catalysed by an enzyme [1]. This is distinct from suppression or down-regulation, which involves a decrease in the amount of enzyme synthesized within living organisms. Therefore, inhibition can be measured both in laboratory settings (in vitro) and within living organisms (in vivo) [2]. When the concentration of an enzyme inhibitor increases, it leads to a decrease in enzyme activity, resulting in a reduction in the amount of product produced. Inhibition of enzyme activity is a crucial regulatory process in living cells and serves as an important diagnostic tool for researchers studying enzymes. Through inhibition studies, researchers can determine the specificity on the enzyme, characteristics of the active site, and the kinetic mechanism governing the reaction.

Such inhibition can have either harmful or beneficial effects. For example, when the metabolism of the antihistamine terfenadine is inhibited by the antibiotic erythromycin or the antifungal ketoconazole, it can lead to potentially dangerous diseases such as arrhythmias and torsades de pointes [3,4]. Conversely,

*For correspondence:

afifi@unimap.edu.my

Received: 20 June 2023

Accepted: 21 Sept. 2023

©Copyright Md Desa. This article is distributed under the terms of the [Creative Commons Attribution License](#), which permits unrestricted use and redistribution provided that the original author and source are credited.

diallyl sulphide, a flavour compound found in garlic oil, can prevent the liver toxicity caused by carbon tetrachloride by inhibiting its metabolism through P450 enzymes [5]. Enzyme inhibition is also a common mechanism of action for many pharmaceuticals. For instance, drugs targeting monoamine oxidase are used to treat depression [6], while inhibition of specific P450 enzymes, such as aromatase involved in steroid biosynthesis, is utilized in the treatment of hormone-dependent diseases like cancer [7, 8].

Three primary types of simple inhibition systems involving a single substrate and a single inhibitor can be identified: competitive inhibition, non-competitive inhibition, and uncompetitive inhibition [9]. Competitive inhibition occurs when a substance, referred to as a competitive inhibitor, binds to the free enzyme in a manner that obstructs the binding of the substrate [10]. In essence, the competitive inhibitor competes with the substrate for the active site of the enzyme. One notable characteristic of competitive inhibitors is that they can be displaced from the active site if high concentrations of the substrate are present, thus restoring the activity of enzyme [11]. Consequently, competitive inhibitors raise the K_M value (Michaelis constant, a parameter used in enzyme kinetics to describe the affinity of an enzyme for its substrate) of a reaction by increasing the concentration of substrate required to saturate the enzyme. However, they do not alter the V_{max} (maximum reaction velocity or the rate when the enzyme is fully saturated with substrate) itself.

On the other hand, non-competitive inhibition involves a substance that binds to an allosteric site on the enzyme, which is distinct from the active site [12]. This binding event reduces the effectiveness of the enzyme, but there is no direct competition between the substrate and the inhibitor for the active site. As a result, the inhibitor does not physically obstruct the substrate-binding site, but it does hinder subsequent reactions. Many non-competitive inhibitors are chemically dissimilar to the substrate, and their inhibition cannot be overcome by increasing the substrate concentration. These inhibitors effectively lower the concentration of active enzyme available in the solution, thereby reducing the V_{max} of the reaction. However, they do not alter the value of K_M .

Lastly, uncompetitive inhibition occurs when an inhibitor specifically binds to the enzyme-substrate complex [13]. As a result, an enzyme-substrate-inhibitor complex is formed, rendering it catalytically inactive. Uncompetitive inhibition is relatively uncommon and occurs when the inhibitor can only bind to the enzyme after the substrate has already bound. Consequently, this type of inhibition is most pronounced at high substrate concentrations and results in a decrease in the V_{max} (maximum reaction rate) of the reaction. Surprisingly, uncompetitive inhibition also leads to a decrease in K_M (Michaelis constant), indicating an increased affinity of the enzyme for its substrate in the presence of the inhibitor. This counterintuitive effect arises because the binding of the inhibitor to the ES complex effectively removes the ES complex, altering the overall reaction equilibrium to favour ES complex formation. It is important to note that since both V_{max} and K_M are reduced, the observed reaction rates in the presence of an uncompetitive inhibitor are always lower than those in its absence.

These three types of inhibition mechanisms provide insights into how different substances can regulate and modulate enzyme activity. Competitive, non-competitive, and uncompetitive inhibitions are all reversible inhibitions, meaning that the inhibitors bind to the enzyme in a reversible manner and can be removed by dialysis or dilution, allowing the enzyme to regain its full activity [11]. Enzyme inhibitors play a crucial role in cells as they are often specific to a particular enzyme and function to regulate its activity. For example, enzymes involved in a metabolic pathway can be inhibited by molecules produced later in the pathway. This inhibition helps reduce the production of molecules that are no longer needed, demonstrating a form of negative feedback. Such feedback mechanisms are essential for maintaining cellular homeostasis, ensuring the balance and proper functioning of cellular processes [12].

Researchers have significantly advanced the field of enzyme kinetics by exploring various inhibition mechanisms and constructing models. These investigations yield profound insights into the intricacies of enzymatic reactions and their inhibition. In a groundbreaking move, [14] introduced a model for enzymatic non-competitive inhibition driven by a product, a dimension often underemphasized in traditional enzyme kinetics. Extending this modelling approach, [15] harnessed model reductions to encompass competitive and uncompetitive inhibition mechanisms, thus underscoring the versatile utility of mathematical modelling. In a comprehensive endeavour, [16] developed a mathematical model that integrates inhibitory, deactivating, and diffusional phenomena to elucidate glucose oxidase kinetics. Departing from the norm, [17] expounded upon enzyme inhibition qualitatively by employing the concepts of the y-intercept and the Lineweaver-Burk plot. In another innovative method, [18] proposed a graphical approach for determining the inhibition constant.

To explore the behaviours of simple inhibition systems within practical reactor settings, the utilization of a prevalent industrial reactor type, specifically the Continuous Stirred-Tank Reactor (CSTR), proves valuable [19]. The CSTR functions in industrial processes by facilitating a consistent flow of reactants through a tank, where they undergo thorough mixing due to the presence of an impeller. This reactor continuously accumulates its output, replenishing its contents with fresh reactants to sustain a uniform volume. Integral reaction parameters, including temperature and pressure, are meticulously controlled, and maintained within the reactor. The fundamental principle governing the operation of a Continuous Stirred-Tank Reactor (CSTR) is the continuous supply of reactants into the reactor, thereby ensuring the uninterrupted progress of the chemical reaction. [20].

One pivotal concern in assessing the safety of a chemical reactor pertains to the identification of scenarios that could lead to undesirable reactor behaviour. A strategy to address this issue involves the identification of multiple stable states and the utilization of this information to devise an effective reactor control strategy [21]. The classical procedure for CSTR, as developed by [22], involves a homogeneous exothermic first-order reaction that occurs in a continuously fed reactor with efficient stirring.

Collectively, these studies enrich our insights on enzyme kinetics and inhibition, providing invaluable tools for probing enzymatic reactions and their associated regulatory networks. The integration of mathematical modelling has led to a more comprehensive understanding of enzyme-catalysed reactions, enabling mechanistic analyses and the identification of factors influencing specificity and catalytic efficiency. However, no comparative analysis exists for these three basic inhibition systems. A notable gap persists in the field due to a lack of rigorous examinations of model stability, particularly with bifurcation analysis. This underscores the need for comprehensive investigation into complex model behaviours, especially within enzyme and biochemical reaction systems. Therefore, this research aims to bridge this gap by modelling simple inhibition systems, studying their parameter-dependent responses, and enhancing our understanding of these complex models within enzyme and biochemical reactions.

Mathematical Models

To represent the model of competitive, non-competitive, and uncompetitive inhibitions, ordinary differential equations (ODEs) are employed. These mathematical models are developed based on several assumptions:

- (a) The density of the reacting mixture remains constant and is not affected by the conversion of substrate to product.
- (b) The volume of the reacting mixture is constant throughout the process.
- (c) Perfect mixing occurs, ensuring that the concentration and temperature inside the reactor are uniform and consistent with the product stream.
- (d) The specific heat of the reacting mixture remains constant and is not influenced by the conversion of substrate to product.
- (e) The heat of reaction (ΔH), which is the energy released or absorbed during the reaction, is constant and independent of temperature and composition.

These assumptions provide a basis for constructing the mathematical models that describe the dynamics of competitive, non-competitive, and uncompetitive inhibitions [23].

Equilibria of Competitive, Non-Competitive, and Uncompetitive Inhibition

In competitive inhibition, the inhibitor and substrate engage in a competition to bind to the enzyme's active site. As a result, they cannot simultaneously occupy the active site, rendering them mutually exclusive [24]. The Figure 1 illustrates competitive inhibition system;

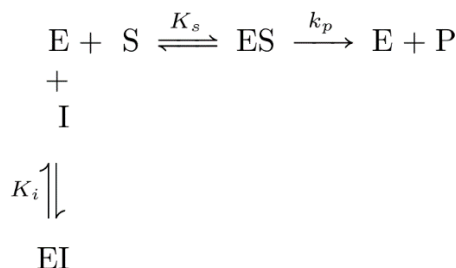


Figure 1. Equilibria of competitive inhibition. E is the enzyme, S is the substrate, ES is the enzyme-substrate complex, EI is the enzyme-inhibitor complex and P is the product

Let $[S]$ the substrate concentration, K_s is the dissociation constant for enzyme-substrate $[ES]$ complex, $[I]$ is the inhibitor concentration, and K_i is the dissociation constant of enzyme-inhibitor $[EI]$ complex. Given that, $K_i = \frac{[E][I]}{[EI]}$, $K_s = \frac{[E][S]}{[ES]}$ and $k_p =$ rate constant for the breakdown of ES to $E+P$. Based on derivation of Michaelis-Menten equation, an expression relating the rate of reaction, r , K_s , $[ES]$, $[I]$ and K_i in the presence of competitor inhibitor can be derived from either rapid equilibrium or steady state assumptions. By using the equation from [9], we can write the rate of reaction as

$$r = \frac{V_{\max} [S]}{K_s \left(1 + \frac{[I]}{K_i} \right) + [S]} \tag{1}$$

where V_{\max} is maximum rate of reaction.

As for the non-competitive inhibition, the Figure 2 describes the relationship between substrate, inhibitor and enzymes.

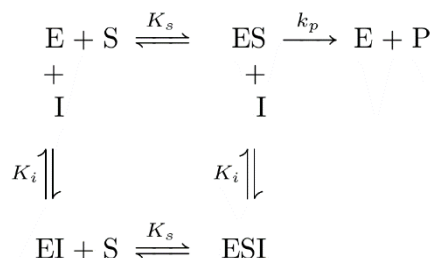


Figure 2. Equilibria of non-competitive inhibition. E is the enzyme, S is the substrate, ES is the enzyme-substrate complex, EI is the enzyme-inhibitor complex, and P is the product

where $[ESI]$ is the enzyme-substrate-inhibitor complex, $K_s = \frac{[E][S]}{[ES]} = \frac{[EI][S]}{[ESI]}$, $K_i = \frac{[E][I]}{[EI]} = \frac{[ES][I]}{[ESI]}$ and $k_p =$ rate constant for the breakdown of ES to $E+P$. By using the same principle of deriving the rate of reaction in Michaelis-Menten equation, [9] has derived the rate of reaction of substrate A for non-competitive inhibition.

$$r = \frac{V_{\max} [S]}{K_s \left(1 + \frac{[I]}{K_i} \right) + [S] \left(1 + \frac{[I]}{K_i} \right)} \tag{2}$$

The General Mass Balance Equation

The general mass balance equation of substrate A and the inhibitor I in a CSTR can be written as

$$\begin{aligned} \frac{dC_A}{dt} &= \frac{F}{V}(C_{A_0} - C_A) - r_A \\ \frac{dC_I}{dt} &= \frac{F}{V}(C_{I_0} - C_I) - r_A \end{aligned} \tag{8}$$

The Energy Balance on CSTR

A general heat balance around a CSTR can be written as

$$\frac{dT}{dt} = \frac{F}{V}(T_0 - T) + \frac{r_A(\Delta H)}{\rho C_p} - \frac{Q(T)}{\rho V C_p} \tag{9}$$

The System of Competitive, Non-competitive and Uncompetitive Inhibition

By substituting the rate of reaction of substrate A , r_A in the general mass balance equation in Eq(8) and energy balance equation in Eq(9), the system of competitive, non-competitive and uncompetitive inhibition can be written as follow.

For competitive inhibition

$$\begin{aligned} \frac{dC_A}{dt} &= \frac{F}{V}(C_{A_0} - C_A) - \frac{k_A e^{-\frac{E}{RT}} C_{ET} C_A}{K_A \left(1 + \frac{C_I}{K_I}\right) + C_A} \\ \frac{dC_I}{dt} &= \frac{F}{V}(C_{I_0} - C_I) - \frac{k_A e^{-\frac{E}{RT}} C_{ET} C_A}{K_A \left(1 + \frac{C_I}{K_I}\right) + C_A} \\ \frac{dT}{dt} &= \frac{F}{V}(T_0 - T) + \frac{k_A e^{-\frac{E}{RT}} C_{ET} C_A}{\rho V C_p \left[K_A \left(1 + \frac{C_I}{K_I}\right) + C_A \right]} - \frac{Q(T)}{\rho V C_p} \end{aligned} \tag{10}$$

For non-competitive inhibition;

$$\begin{aligned} \frac{dC_A}{dt} &= \frac{F}{V}(C_{A_0} - C_A) - \frac{k_A e^{-\frac{E}{RT}} C_{ET} C_A}{K_A \left(1 + \frac{C_I}{K_I}\right) + C_A \left(1 + \frac{C_I}{K_I}\right)} \\ \frac{dC_I}{dt} &= \frac{F}{V}(C_{I_0} - C_I) - \frac{k_A e^{-\frac{E}{RT}} C_{ET} C_A}{K_A \left(1 + \frac{C_I}{K_I}\right) + C_A \left(1 + \frac{C_I}{K_I}\right)} \\ \frac{dT}{dt} &= \frac{F}{V}(T_0 - T) + \frac{k_A e^{-\frac{E}{RT}} C_{ET} C_A}{\rho V C_p \left[K_A \left(1 + \frac{C_I}{K_I}\right) + C_A \left(1 + \frac{C_I}{K_I}\right) \right]} - \frac{Q(T)}{\rho V C_p} \end{aligned} \tag{11}$$

And lastly for uncompetitive inhibition

$$\begin{aligned} \frac{dC_A}{dt} &= \frac{F}{V}(C_{A_0} - C_A) - \frac{k_A e^{-\frac{E}{RT}} C_{ET} C_A}{K_A + C_A \left(1 + \frac{C_I}{K_I}\right)} \\ \frac{dC_I}{dt} &= \frac{F}{V}(C_{I_0} - C_I) - \frac{k_A e^{-\frac{E}{RT}} C_{ET} C_A}{K_A + C_A \left(1 + \frac{C_I}{K_I}\right)} \\ \frac{dT}{dt} &= \frac{F}{V}(T_0 - T) + \frac{k_A e^{-\frac{E}{RT}} C_{ET} C_A}{\rho V C_P \left[K_A + C_A \left(1 + \frac{C_I}{K_I}\right) \right]} - \frac{Q(T)}{\rho V C_P} \end{aligned} \tag{12}$$

Dimensionless Equation

We can define the dimensionless variable as $y = \frac{C_A}{C_{A_0}}, z = \frac{C_I}{C_{I_0}}, D = \frac{F}{V}$ and $\tau = Dt$. For the dimensionless parameter, let $\varepsilon = \frac{C_{ET}}{C_{A_0}}, C_1 = \frac{K_A}{C_{A_0}}, C_2 = \frac{K_I}{C_{I_0}}$ and $C_3 = \frac{C_{I_0}}{C_{A_0}}$. As for energy balance in Eq(9), multiply both sides of equation with $\frac{V \rho C_P}{FC_{A_0}(\Delta H)}$.

$$\begin{aligned} \frac{dT}{dt} \left(\frac{V \rho C_P}{FC_{A_0}(\Delta H)} \right) &= \frac{\rho C_P}{C_{A_0}(\Delta H)} T_0 - \frac{\rho C_P}{C_{A_0}(\Delta H)} T + \frac{r_A}{C_{A_0}} \left(\frac{V}{F} \right) \\ &\quad - \frac{Q(T)}{FC_{A_0}(\Delta H)} \end{aligned} \tag{13}$$

Let $\theta = \frac{\rho C_P T}{C_{A_0}(\Delta H)}$ and $\theta_0 = \frac{\rho C_P T_0}{C_{A_0}(\Delta H)}$. From θ , we get $T = \frac{\theta C_{A_0}(\Delta H)}{\rho C_P}$. Substitute T into Arrhenius equation in Eq(13) and upon rearranging, we can group these parameters into dimensionless parameter, $\beta = \frac{E \rho C_P}{RC_{A_0}(\Delta H)}$. For the heat controller function $q(\theta) = \frac{Q(T)}{FC_{A_0}(\Delta H)}$, by using the proportional control constant from [25], we can define $q(\theta) = U(\theta - \theta_c)[1 + K_c(\theta - \theta_s)]$. Finally, we can substitute the dimensionless variables y, z, θ and τ and the dimensionless parameters $D, \theta_0, \theta_c, \theta_s, \varepsilon, C_1, C_2, C_3, q(\theta)$ and β into Eq(10), Eq(11) and Eq.(12). The final equations to be further analysed are;

Competitive Inhibition:

$$\begin{aligned} \frac{dy}{d\tau} &= 1 - y - \frac{k_A e^{-\frac{\beta}{\theta}} \epsilon y}{D \left[C_1 \left(1 + \frac{z}{C_2} \right) + y \right]} \\ \frac{dz}{d\tau} &= 1 - z - \frac{k_A e^{-\frac{\beta}{\theta}} \epsilon y}{C_3 D \left[C_1 \left(1 + \frac{z}{C_2} \right) + y \right]} \\ \frac{d\theta}{d\tau} &= \theta_0 - \theta + \frac{k_A e^{-\frac{\beta}{\theta}} \epsilon y}{D \left[C_1 \left(1 + \frac{z}{C_2} \right) + y \right]} - U(\theta - \theta_c) [1 + K_c (\theta - \theta_s)] \end{aligned} \tag{14}$$

Non-competitive inhibition

$$\begin{aligned} \frac{dy}{d\tau} &= 1 - y - \frac{k_A e^{-\frac{\beta}{\theta}} \epsilon y}{D \left(1 + \frac{z}{C_2} \right) (C_1 + y)} \\ \frac{dz}{d\tau} &= 1 - z - \frac{k_A e^{-\frac{\beta}{\theta}} \epsilon y}{C_3 D \left(1 + \frac{z}{C_2} \right) (C_1 + y)} \\ \frac{d\theta}{d\tau} &= \theta_0 - \theta + \frac{k_A e^{-\frac{\beta}{\theta}} \epsilon y}{D \left(1 + \frac{z}{C_2} \right) (C_1 + y)} - U(\theta - \theta_c) [1 + K_c (\theta - \theta_s)] \end{aligned} \tag{15}$$

and for Uncompetitive Inhibition;

$$\begin{aligned} \frac{dy}{d\tau} &= 1 - y - \frac{k_A e^{-\frac{\beta}{\theta}} \epsilon y}{D \left[C_1 + y \left(1 + \frac{z}{C_2} \right) \right]} \\ \frac{dz}{d\tau} &= 1 - z - \frac{k_A e^{-\frac{\beta}{\theta}} \epsilon y}{C_3 D \left[C_1 + y \left(1 + \frac{z}{C_2} \right) \right]} \\ \frac{d\theta}{d\tau} &= \theta_0 - \theta + \frac{k_A e^{-\frac{\beta}{\theta}} \epsilon y}{D \left[C_1 + y \left(1 + \frac{z}{C_2} \right) \right]} - U(\theta - \theta_c) [1 + K_c (\theta - \theta_s)] \end{aligned} \tag{16}$$

Results and Discussion

In this section, we will commence by showcasing the result phase portrait analysis for each system. Subsequently, we will delve into a comprehensive bifurcation analysis, encompassing the impact of the dilution rate and the enzyme concentration proportional control constant. Finally, we will present the codimension two parameter bifurcation analysis, followed by a discussion.

Phase Portrait Analysis

The models consist of three ordinary differential equations describing the dynamics of 3 enzymatic reactions with inhibitor in a CSTR. Three variables in this model are y, z and θ , which represent

substrate concentration, inhibitor concentration and reactor temperature. All parameter values used in this study are listed in Table 1. In this section, we present the phase portrait analysis of each model.

Table 1. The variables and parameters of the simple inhibition models

| Variable/Parameter | Description | Value | Reference |
|--------------------|---|------------------------|-----------|
| y | Dimensionless concentration of substrate | - | |
| z | Dimensionless concentration of inhibitor | - | |
| θ | Dimensionless temperature of the reactor the stability of reaction | - | |
| τ | Dimensionless time | - | |
| k_A | Reaction velocity constant | e^{25} | [26] |
| ε | Dimensionless total enzyme concentration | $0 < \varepsilon < 30$ | [26] |
| D | Dilution rate: the rate that the existing medium in the reactor is replaced by a fresh medium | $0 \leq D \leq 10$ | [26] |
| β | Dimensionless parameter for heat transfer | 50 | [26] |
| θ_0 | Dimensionless initial reactor temperature on the stability of the reaction | 1.75 | [26] |
| θ_c | Dimensionless mean temperature of water in the cooling coil | 1.75 | [26] |
| θ_s | Desired steady-state temperature | 2 | [26] |
| U | Dimensionless analogue of U_0A , the overall heat transfer rate | 1 | [26] |
| K_C | Proportional control on the cooling water flow rate constant | $1 \leq K_C \leq 12$ | [26] |
| C_1 | Dimensionless Michaelis-Menten constant | 0.1 | [18] |
| C_2 | Dimensionless dissociation constant for enzyme-inhibitor complex | 0.1 | [18] |
| C_3 | Ratio of initial concentration of inhibitor and substrate | 7.11 | [18] |

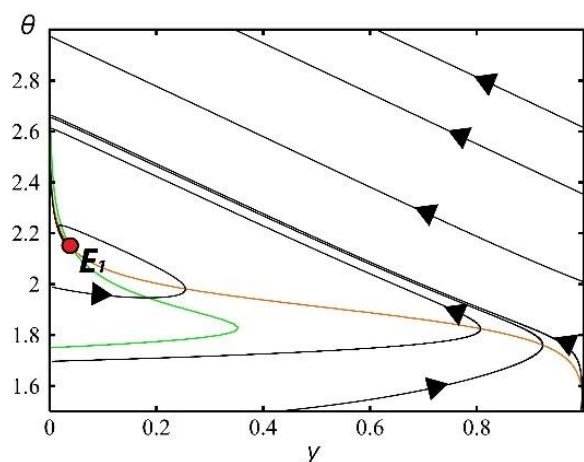
The XPPAUT program is utilized to generate the phase portrait for each system. In order to showcase the unique characteristics of each model, we solve the ODE systems numerically and create the phase portrait, representing the substrate concentration on the x-axis and the reactor temperature on the y-axis. Multiple initial conditions are employed to trace the trajectories of the solutions. These phase portraits facilitate our comprehension of the potential behaviours exhibited by the solutions and the underlying mechanisms responsible for these diverse behaviours.

The dynamics of a CSTR are influenced by certain parameters, namely the dilution rate or residence time [27], enzyme concentration [28] and reactor temperature [29]. The dilution rate, quantified as the ratio of incoming substrate flow to the reactor's volume [30], plays a pivotal role by directly determining the duration for which the liquid remains exposed to the operational conditions of reactor and chemical processes. Meanwhile, the temperature of the CSTR is a fundamental determinant impacting the reaction kinetics within the system [31]. The proportional control constant, denoted as K_C , plays a central function in the regulation of the rate at which thermal energy dissipates from the reactor. This regulation primarily occurs through the supervision and adjustment of the flow of coolant water. Concurrently, the concentration of enzymes significantly influences the behaviour of exothermic biocatalytic reactions, with a direct bearing on the economic implications of the process [32]. Striking an optimal balance between achieving desirable reaction rates, conversion efficiency, and effective management of enzyme costs becomes imperative for maximizing the economic viability of the overall biocatalytic process.

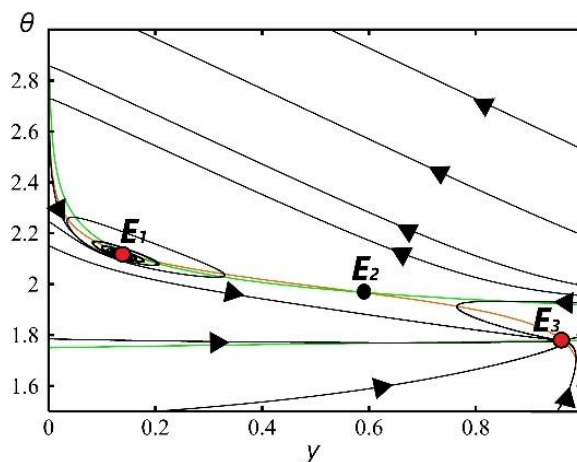
In this investigation, our main goal is to assess the effect of varying dilution rates, D and proportional control constants, K_C while keeping enzyme concentration, ε constant. The primary objective is to observe and analyse the diverse behaviours exhibited by each system as the parameters D and K_C are varied. Given the qualitative similarities in behaviours observed across all three models at different D and K_C values, we present the phase portrait of the competitive inhibition system in Figure 4. We can discern four distinct types of dynamics within this system: (i) the presence of a stable equilibrium, (ii)

bistability characterized by the existence of two equilibriums, (iii) bistability between a stable equilibrium and a stable limit cycle, and (iv) the presence of a limit cycle.

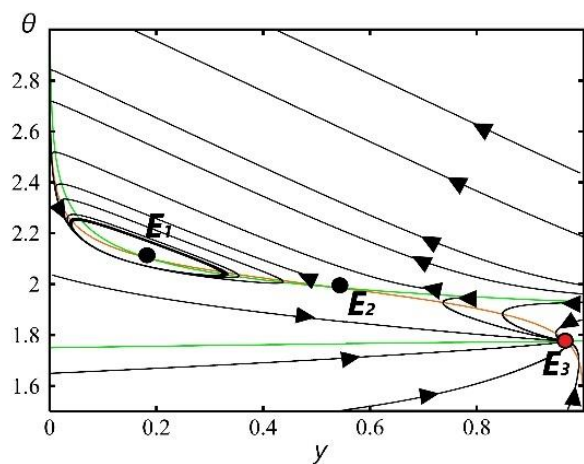
In Figure 4(a), there is a stable node, denoted as E_1 , when $D=1$ and $K_C=3$. This equilibrium point attracts all trajectories within the quadrant. At this steady-state condition, the concentration of substrate, y , is relatively small, while the temperature of the reactor is close to the desired value. This suggests that the substrate's reliance on the inhibitor is inexplicable, and consequently, most substrates in the CSTR will be catalysed by the enzyme. This statement is supported by [33], particularly state that, as dilution rates decrease, there is a tendency for enzyme activity to rise and thereby substantiating the previously mentioned observation.



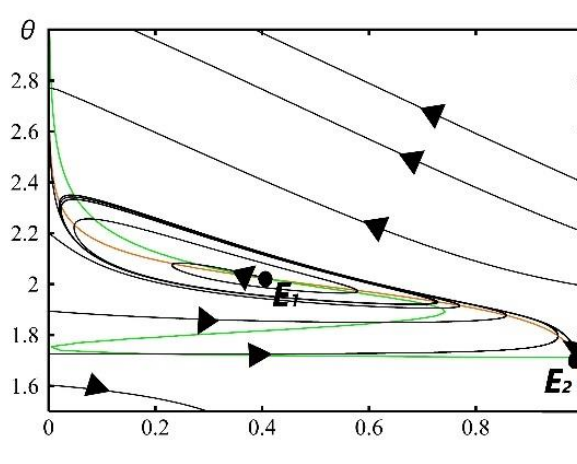
(a) $D=1, K_C=3$



(b) $D=2.8, K_C=3$



(c) $D=3, K_C=3$



(d) $D=3, K_C=8$

Figure 4. Phase portrait of competitive inhibition with four different values of dilution rate, D , and proportional control constant, K_C with a constant enzyme concentration $\varepsilon = 5$. The steady states are marked by black or red filled circle. Red circle is stable steady-state while black circle is unstable steady-state. Green and yellow line are nullclines of the plane. x -axis is dimensionless concentration of substrate and y -axis is the dimensionless temperature of the reactor. Arrows indicate the direction of the trajectories for different initial conditions.

Figure 4(b) demonstrates the emergence of bistability in the system when D is raised to 2.8. This bistability is characterized by the presence of two stable steady-states: E_1 and E_3 . The equilibrium point E_2 , which represents the stable manifold of the saddle-type solution, acts as a boundary separating the basins of attraction for E_1 and E_3 . Depending on the initial conditions, trajectories will converge towards either E_1 or E_3 . These changes in dynamics indicate that an increase in the dilution rate, D , can lead to the occurrence of bistability. The stable steady-state E_1 is associated with a lower substrate concentration, indicating that the inhibitor has minimal impact on the enzyme-substrate reaction. Conversely, the stable steady-state E_3 is observed at a higher substrate concentration, suggesting that the inhibitor effectively suppresses the biocatalytic reaction by competing with the substrate.

When $D=3$ and $K_C=3$, as depicted in Figure 4.1(c), a different type of phenomenon occurs, characterized by alternate stable states. Specifically, there is a bistability between a stable limit cycle and a stable steady-state. The previous attractor at E_1 now transforms into a stable limit cycle, while E_3 remains a stable steady-state. The equilibrium point E_2 , which represents the stable manifold of the saddle-type solution, divides the basins of attraction for E_1 and E_3 . The system's behaviour is determined by its initial conditions. When managing the CSTR, it is crucial to consider the transition from a stable steady-state to a stable limit cycle at E_1 . As illustrated in Figure 4.1(b) and Figure 4.1(c), even a small increase in the dilution rate D can cause a stable steady-state to transform into a limit cycle, where the substrate concentration oscillates with a certain amplitude. Such oscillations may not be desirable for certain biocatalytic processes. On the other hand, the alternative stable steady-state E_3 exhibits a higher substrate concentration, indicating that the inhibitor has effectively slowed down the biocatalytic activity.

Figure 4.1(d) demonstrates an increase in the proportional control constant, K_C , from 3 to 8. This adjustment was made to simulate an increment in the heat dissipation process, given the critical role of K_C in controlling the rate of heat dissipation from the reactor, primarily through the control and adjustment of cooling-water flow. As a result, the size of the stable limit cycle observed in the previous case has significantly increased. Additionally, the stable steady-state observed in the previous cases has diminished, leaving the limit cycle as the sole attractor of the system.

The phase portrait analysis provides insights into the dynamical outcomes of the models, which can be summarized as follows: (i) Varying the magnitude of the dilution rate, D , or the proportional control constant, K_C , can lead to the emergence of bistability phenomena, where the system exhibits two stable states. (ii) Changes in the magnitudes of these chemically relevant parameters can result in the appearance of a stable limit cycle, indicating sustained oscillations in the system. (iii) Increasing the value of D or K_C can cause the stable steady-state behaviour to cease to exist, suggesting that higher values of these parameters disrupt the stability of the system. These findings highlight the significant impact that altering the characteristics of the system can have on its dynamical behaviour.

One Parameter Bifurcation Analysis

To unravel the underlying mechanisms driving the diverse observations within the CSTR system, we conducted a codimension one bifurcation analysis using Auto in XPPAUT. This systematic analysis involved the deliberate variation of three critical parameters: (i) the dilution rate, D (ii) the enzyme concentration, ε and (iii) the proportional control constant, K_C . These parameters hold pivotal roles in shaping the dynamics of biocatalytic systems. Investigating the influence of D, ε and K_C within the context of different inhibition mechanisms is crucial for better understanding of enzyme kinetics and its practical applications. By systematically examining and varying these parameters, our objective was to gain insights into these distinct biochemical processes impact the dynamics of the system, thereby elucidating the observed behaviours illustrated in our analysis of phase plane.

Effect of Dilution Rate

The dilution rate plays a pivotal role in the operation of a Continuous Stirred Tank Reactor

(CSTR). The dilution rate, D refers to the speed at which fresh medium replaces the existing medium within the reactor. This rate directly influences the duration for which the substrate and the inhibitor remain inside the reactor before being discharged. Analysing the phase portrait diagrams depicted in Figure 4, it becomes evident that the variation of the dilution rate, D holds significant importance in understanding how the system dynamics evolve, particularly through codimension-one bifurcation analysis. By employing a codimension-one bifurcation, we gain insights into various aspects, including the emergence of oscillations, the existence of stable steady-state regions, the occurrence of bistability, and the specific parameter values at which these transitions occur. Figure 5 visually presents the outcomes obtained from the codimension-one bifurcation analysis.

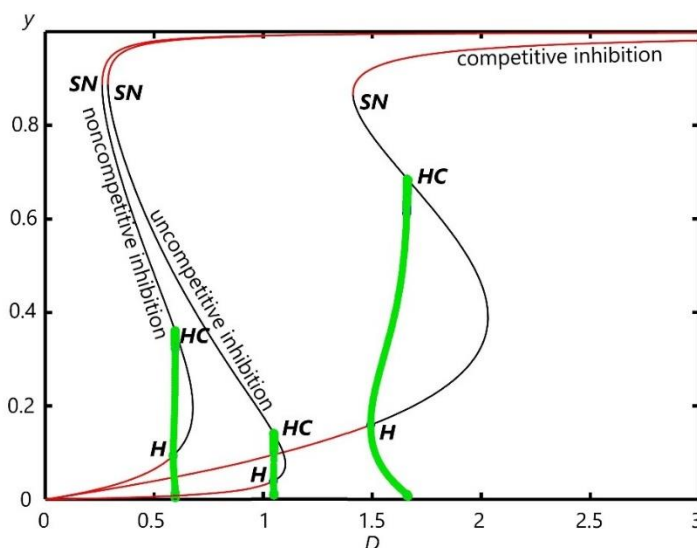


Figure 5. Bifurcation diagram with D as the bifurcation parameter. SN is a saddle node bifurcation, H is a Hopf bifurcation and HC is a homoclinic bifurcation. Red (black) curve corresponds to stable (unstable) equilibrium. The green curve corresponds to the amplitude of limit cycle

This plot has been generated by keeping $\varepsilon = 3$ and $K_C = 5$, while the other parameters are set according to Table 1. Upon analyzing this diagram, several intriguing observations can be made. The three systems exhibit qualitatively similar branches of attractors, each with three distinct bifurcation points marking significant changes in their dynamics. The first bifurcation point, known as the saddle node bifurcation (SN), occurs when the upper branch (red curve) steady-state collides with the middle branch (black curve) steady-state. In the lower region of the y -axis, a stable limit cycle emerges from the stable steady-state at a critical point called H , representing a Supercritical Hopf bifurcation. This stable limit cycle continues until it reaches another critical point, HC , where a homoclinic bifurcation occurs. The homoclinic bifurcation is triggered when the limit cycle's amplitude intersects with the unstable saddle point in the middle branch (black curve).

Upon closer inspection of these three bifurcation curves, it becomes evident that there are two regions of bistability and two regions characterized by stable steady-states. The first bistability phenomenon occurs between the two stable steady-states and is observed within the range of $SN < D < H$. The second observation of bistability arises between a stable steady-state and a stable limit cycle, and it occurs when $H < D < HC$. On the other hand, two regions exhibiting stable steady-states are observed when $D < SN$ and $D > HC$.

In simple inhibition systems, it is observed that the substrate concentration exhibits distinct patterns at different dilution rates. At low dilution rates, such as $D = 0.5$, the substrate concentration is significantly lower, approaching zero. Conversely, at higher dilution rates ($D > 2$), the substrate concentration becomes exceptionally high, nearing a value of 1. As the dilution rate increases, the substrate concentration generally increases as well. However, once a certain threshold (SN) is surpassed, a dramatic change in the substrate concentration occurs, leading to the emergence of bistability. This bistable behaviour is attributed to the occurrence of a saddle node bifurcation. Depending on the initial conditions, the substrate concentration can either

exhibit a rapid increase or a gradual rise. This phenomenon can be explained by the regulation of the CSTR's inflow and outflow, which are controlled by the dilution rate. At lower dilution rates, the inflow and outflow rates of the CSTR are minimized, resulting in a longer residence time for the substrate and inhibitor within the reactor. This extended duration increases the likelihood of substrate and inhibitor molecules accessing the active site of the enzyme, thereby influencing the probability of substrate catalysis or inhibition.

Another notable finding is that competitive inhibition exhibits higher dilution rate thresholds (such as SN , H and HC) compared to other inhibition models, namely uncompetitive and non-competitive inhibition. Furthermore, competitive inhibition displays a larger amplitude of oscillation and a wider range for the limit cycle when compared to non-competitive and uncompetitive inhibitions. This discrepancy can be attributed to the nature of competitive inhibition, which involves a genuine competition between the substrate and inhibitor for the same active site on the enzyme. This competitive mechanism leads to an increase in the apparent K_M (the substrate concentration required to achieve half of the maximum reaction rate, V_{max}), while the V_{max} value remains unchanged. Consequently, the threshold values (SN , H and HC) for competitive inhibition are greater than those for non-competitive and uncompetitive inhibitions. It is important to note that all systems exhibit bistability; however, uncompetitive inhibition appears to have a wider range of bistability, particularly in the lower range of dilution rate, D .

Effect of Enzyme Concentration

The parameter ε in the context of this study represents the total number of cells or enzymes concentration present within the reactor. Enzymes play a crucial role in biocatalytic processes as they regulate the reaction rate. In the case of a simple inhibition system, the substrate and inhibitor engage in a competitive interaction for the active site or allosteric site on the enzyme molecule. In this section, we will explore the impact of varying the enzyme quantity in an enzyme-catalysed reaction. To ensure favourable outcomes, it is important to maintain lower levels of both the dilution rate, D , and the proportional control constant, K_c . Therefore, for this K_c study, the dilution rate is set at 3 and the proportional control constant is set at 5. The remaining parameters can be found in Table 1.

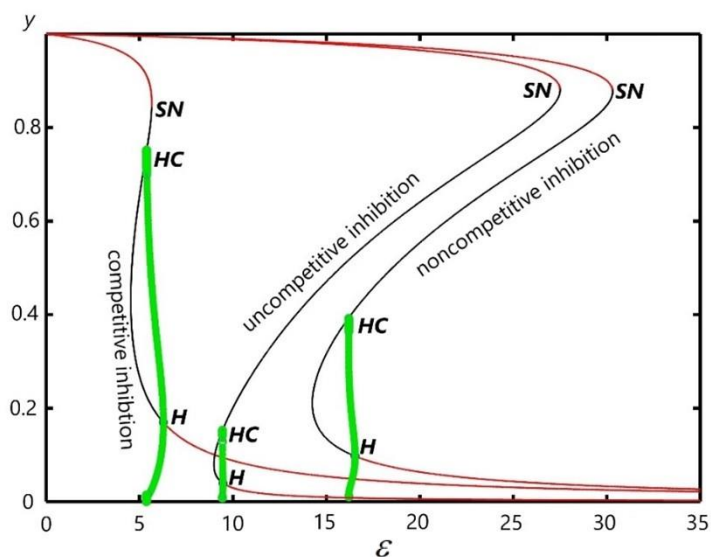


Figure 6. Bifurcation diagram with ε as the bifurcation parameter. SN is a saddle node bifurcation, H is a Hopf bifurcation and HC is a homoclinic bifurcation. Red (black) curve corresponds to stable (unstable) equilibrium. The green curve corresponds to the amplitude of limit cycle

The bifurcation diagram depicted in Figure 6 illustrates the effects of competitive, non-competitive, and uncompetitive inhibitions as the parameter ε is varied. Interestingly, this bifurcation diagram exhibits a nearly mirrored image of the bifurcation diagram with D as the bifurcation parameter. Specifically, the

shape of the curve in Figure 6 is inverted compared to the previous diagram. All systems, regardless of the type of inhibition, exhibit qualitatively similar behaviour with three critical points: SN , H and HC . These critical points mark the locations where significant dynamical changes occur. In the lower branch of the substrate concentration, y , a stable limit cycle emerges from the stable steady-state at a critical point denoted as H , indicating the presence of a Hopf bifurcation. This stable limit cycle continues until it reaches the critical point HC , where a homoclinic bifurcation occurs. The homoclinic bifurcation arises due to the collision of the limit cycle's amplitude with the unstable saddle point in the middle branch (black curve).

When comparing the current bifurcation diagram in Figure 6 to the previous one in Figure 5, it is evident that only the non-competitive and uncompetitive inhibition systems exhibit two regions of bistability and two regions of stable steady-state. The first bistability phenomenon occurs between the two stable steady-states and is observed when $SN < \varepsilon < H$. The second bistability phenomenon occurs between a stable steady-state and a stable limit cycle and is observed in the region where $H < \varepsilon < HC$. On the other hand, two regions characterized by stable steady-states are observed when ε is less than HC and when ε is greater than SN . In the case of competitive inhibition, the bistability phenomenon only occurs in the region of $SN < \varepsilon < HC$, where both a stable steady-state and a stable limit cycle are present. In the regions where $\varepsilon < HC$ and $\varepsilon > H$, only a stable steady-state is observed. These observations can be explained by the underlying mechanisms of these three systems. As observed in Figure 5, when the dilution rate is set to $D=3$, the substrate concentration in competitive inhibition is significantly lower than that in non-competitive and uncompetitive inhibitions. In this scenario, competitive inhibition outperforms non-competitive and uncompetitive inhibition in terms of substrate catalysis. Consequently, the threshold values for competitive inhibition (SN , H and HC) are lower compared to non-competitive and uncompetitive inhibitions when the enzyme concentration, ε , is varied. Furthermore, in the non-competitive inhibition system, the maximum velocity of the reaction, V_{max} , decreases, causing the enzyme to become saturated more quickly than in competitive and uncompetitive inhibition systems. This indicates that a higher enzyme concentration is required to achieve the desired conversion. As a result, the critical point values (SN , H and HC) for non-competitive inhibition are higher than those for competitive and uncompetitive inhibition.

The concentration of enzymes plays a crucial role in determining the outcomes of a system, as evident from the bifurcation diagram. When there is no enzyme present ($\varepsilon = 0$), the substrate concentration reaches its maximum level. In this scenario, no reaction takes place in the reactor since there are no active sites available for substrate or inhibitor binding. As the enzyme concentration increases, more active sites become available for substrate and inhibitor binding. To achieve a high conversion rate, it is necessary to increase the enzyme concentration up to the threshold limit represented by the H point. At this point, the substrate concentration exceeds the oscillation region indicated by the green curve. However, further increases in enzyme concentration beyond the H point result in a decrease in the substrate concentration. This becomes inefficient and wasteful as the substrate concentration decreases very slowly. It is sufficient to operate around or near the H point to achieve higher conversion rates. Using the H point as the optimal enzyme concentration can be advantageous, as increasing the enzyme concentration beyond this point may lead to higher operational costs without significant improvements in the conversion rate.

Effect of Proportional Control Constant

In this section, our objective is to examine the implications of varying the proportional control constant, K_c , on the overall dynamics of the system. In exothermic reactions, the temperature within the reactor holds utmost significance. As the reaction progresses, the temperature tends to rise, necessitating the removal of excessive heat to maintain system stability and ensure an optimal temperature range for the functioning of the enzyme. The proportional control constant, K_c , assumes a critical role as it control the rate at which heat is dissipated from the reactor through the regulation of cooling-water flow. Therefore, it is crucial to understand the significant influence of temperature control on the reaction system. A higher value of K_c allows for more effective heat dissipation, resulting in lower reactor temperatures.

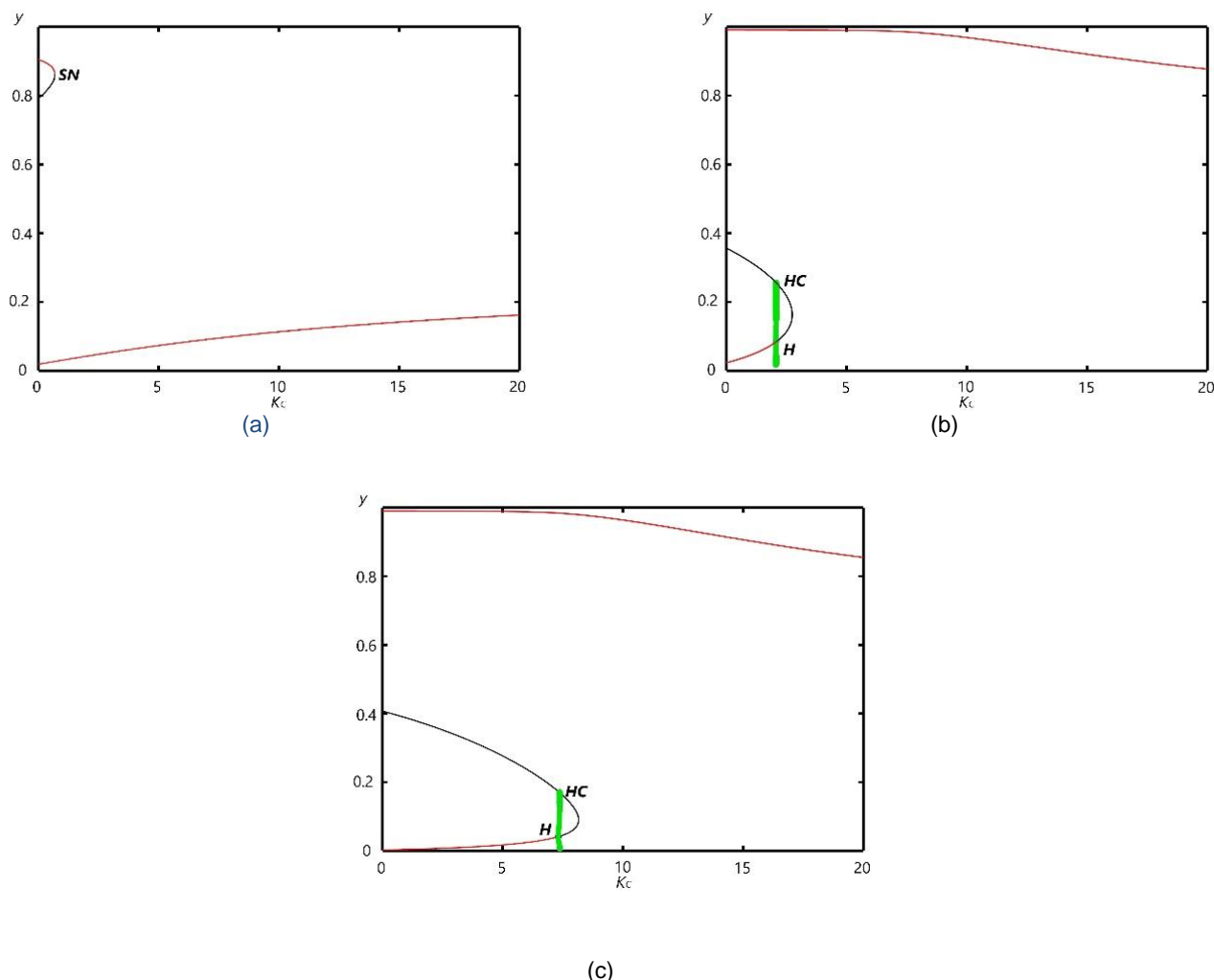


Figure 7. Bifurcation diagrams with K_c as bifurcation parameter. SN is a saddle node bifurcation, H is a Hopf bifurcation and HC is a homoclinic bifurcation. Red (black) curve corresponds to stable (unstable) equilibrium. The green curve corresponds to the amplitude of limit cycle. (a) Competitive inhibition. (b) Non-competitive inhibition. (c) Uncompetitive inhibition

To explore the behaviour of these systems under varying proportional control constant, we set $\varepsilon = 7$ and $D=2$. The remaining parameter values can be found in Table 1. Figure 7 presents the bifurcation diagram for simple inhibition systems, with K_c as the bifurcation parameter. In the case of competitive inhibition, there is only one critical point, SN . On the other hand, both non-competitive and uncompetitive inhibitions exhibit similar curves with two critical points, H and HC . At the critical point H , which corresponds to a Hopf bifurcation, a stable limit cycle emerges from the stable steady-state in the lower range of y . This stable limit cycle terminates at the critical point HC , where a homoclinic bifurcation occurs.

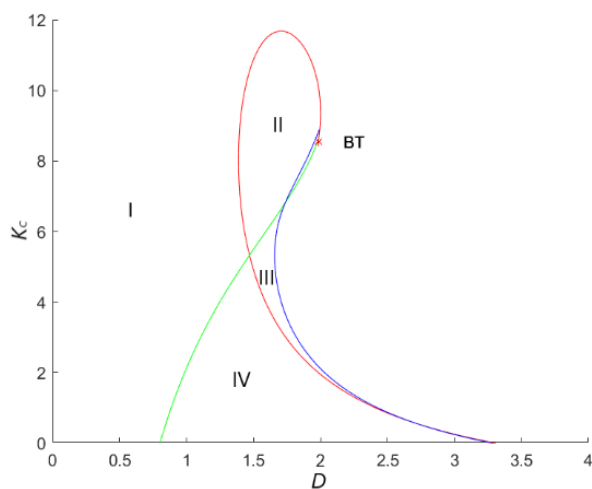
In the range of low proportional control constant values, K_c , all systems exhibit a phenomenon of bistability characterized by the presence of two stable steady-states. Among the three types of inhibitions, non-competitive inhibition shows the largest region of bistability, followed by competitive inhibition, and finally uncompetitive inhibition. In the case of competitive inhibition, the bistability region disappears when K_c exceeds the critical point SN , resulting in a system with only a single stable state. However, for non-competitive and uncompetitive inhibitions, another region of bistability emerges between the critical points H and HC , provided that $H < K_c < HC$. This region is marked by the coexistence of a stable steady-state and a stable

limit cycle. Beyond $K_C > HC$, both non-competitive and uncompetitive inhibition systems exhibit a single stable state. The disappearance of the bistability phenomenon with increased heat removal, as reflected by higher K_C values, highlights the significance of efficient heat removal in enzymatic reactions. Bistability can be undesirable in such systems, and efforts are made to eliminate it [34].

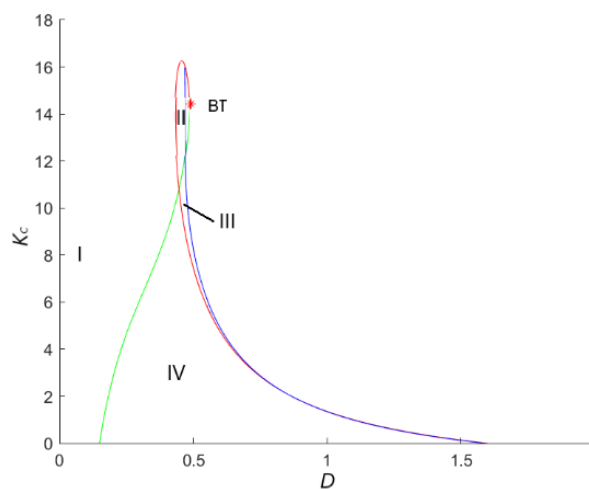
Compared to non-competitive and uncompetitive inhibitions, competitive inhibition demonstrates a notable decrease in substrate concentration at higher values of the proportional control constant, K_C (e.g., $K_C > 10$). This finding suggests that increased heat removal, represented by higher K_C values, has a significant influence on the competitive inhibition system. It results in a reduction of substrate concentration in the final product. In contrast, for non-competitive and uncompetitive inhibitions, the effect of higher K_C values is opposite. It leads to a decrease in substrate concentration on the upper branch of the bifurcation diagram. However, once K_C exceeds the critical point HC , the lower branch of stable steady-states is eliminated. Consequently, the subsequent stable attractor is shifted to the upper branch. This phenomenon should be carefully considered when operating a continuous stirred-tank reactor (CSTR) for systems such as non-competitive and uncompetitive inhibitions.

Codimension Two Bifurcation Analysis

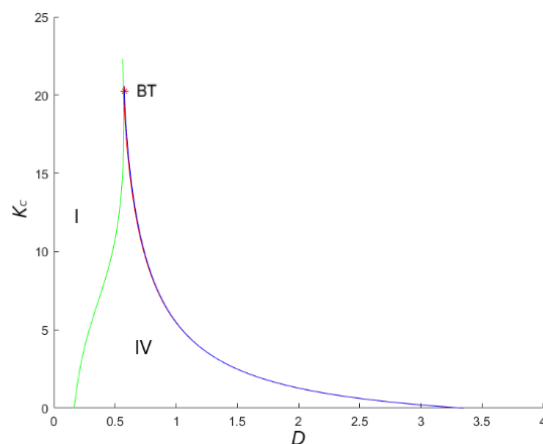
In this section, we will investigate the interplay between two key parameters, the dilution rate, D and the proportional control constant K_C , to examine their effects on the dynamics of the inhibition systems. To visualize these effects, we will utilize a codimension two bifurcation diagram that provides insights into how the system dynamics evolve as both D and K_C are varied. This diagram will shed light on the complex interactions and transformations that occur within the three inhibition systems.



(a)



(b)



(c)

Figure 8. Codimension two bifurcation diagrams with D and K_c as bifurcation parameters. The green curves are saddle node bifurcation continuation, red curves are Hopf bifurcation continuation and blue curves are homoclinic bifurcation continuation. BT is a Bogdanov-Taken bifurcation. (a) Codimension two bifurcation diagram of competitive inhibition. (b) Codimension two bifurcation diagram of non-competitive inhibition. (c) Codimension two bifurcation diagram of uncompetitive inhibition

Figure 8 displays distinct regions that correspond to different dynamics observed in the phase portraits of Figure 4. In region I, a single stable steady-state is observed, which aligns with the phase portrait depicted in Figure 4(a). Moving into region II, a stable limit cycle becomes prominent, as shown in the associated phase portrait of Figure 4(d). Region III signifies the presence of bistability, where both steady-states and limit cycles coexist, as depicted in Figure 4(c). Lastly, region IV denotes bistability between two stable steady-states, as illustrated in Figure 4(b).

The qualitative similarities in the dynamics of the enzymatic reaction systems are evident across all three types of inhibition. However, the extent of their dynamical changes varies. Competitive and non-competitive inhibitions exhibit all four regions (I, II, III, and IV), with regions II and III being more prominent in competitive inhibition. In contrast, uncompetitive inhibition only displays regions I and IV. To understand why only these regions are present in uncompetitive inhibition, Figure 5 and Figure 7 provide valuable insights. In both figures, the Hopf bifurcation point (H) and the homoclinic bifurcation point (HC) for uncompetitive inhibition are closely located. The corresponding bifurcation curves (red for Hopf bifurcation and blue for homoclinic bifurcation) are tightly intertwined as the dilution rate and proportional control constant are simultaneously varied. This tight coupling between the two bifurcation points leads to the emergence of only regions I and IV in the uncompetitive inhibition system.

The codimension two bifurcation diagrams presented illustrate three notable characteristics. Firstly, the phenomenon of bistability is observed in all systems. At lower dilution rates, a single stable steady-state is evident. However, as the dilution rate is significantly increased, a second attractor emerges, leading to bistability between the two stable steady-states. Secondly, the impact of increasing heat removal is apparent. With higher rates of heat removal, the system undergoes a transition to a single stable state, eliminating the presence of bistability. Lastly, the effect of increasing the dilution rate is observed. As the dilution rate is progressively raised, the system converges to a single steady-state, thereby eliminating the possibility of bistability.

Discussion

Previous studies, such as those conducted by [35]–[37] have extensively explored the influence of dilution rate (residence time) in continuous stirred-tank reactors (CSTRs). The findings from these studies align with the bifurcation diagram presented in our study when considering variations in the dilution rate. However, it is important to note that in contrast to our study, Uppal *et al.* (1976) observed a decrease in the concentration on the upper branch with large values of D due to the cooling effect. In our investigation, we observed that all systems exhibited similar characteristics as the dilution rate increased,

with the substrate concentration also increasing. Notably, competitive inhibition demonstrated higher threshold values (SN, H and HC) compared to the other systems, indicating its unique behaviour in response to changes in the dilution rate.

The findings of our study are consistent with the research conducted by [38] regarding the variation of enzyme concentration. Our results confirm that increasing the enzyme concentration leads to improved substrate conversion. Notably, we identified the Hopf bifurcation point (H) as the threshold for enzyme concentration. When the enzyme concentration falls below the Hopf point, the substrate concentration increases or, in some cases, may oscillate. Therefore, it is recommended to increase the enzyme concentration beyond the Hopf limit in order to achieve higher substrate conversion rates. Furthermore, our study highlights that the competitive inhibition system exhibits lower threshold values (SN, H , and HC) compared to the non-competitive and uncompetitive inhibition systems. This suggests that competitive inhibition requires a lower enzyme concentration than the other two systems to achieve optimal substrate conversion. These findings emphasize the importance of considering the specific inhibition mechanism and its impact on the enzyme concentration requirements for efficient substrate conversion.

The importance of temperature regulation in the operation of a CSTR, particularly for exothermic systems, has been emphasized in previous research, such as the study conducted by [39]–[42]. Neglecting the dynamics of temperature control can lead to hazardous situations. In our study, we applied bifurcation analysis to investigate the impact of the proportional control constant, K_c on the system dynamics, given its role in regulating the dissipation of heat from the reactor. Our findings demonstrate that all three systems exhibit two equilibria at lower values of K_c . This indicates the presence of bistability, where two stable steady-states coexist. The critical point for bistability is reached when the proportional control constant is within a certain range. The effect of increased heat removal at higher K_c values vary depending on the inhibition mechanism. In the case of competitive inhibition, higher heat removal leads to a decrease in substrate concentration in the end product. On the other hand, for non-competitive and uncompetitive inhibitions, increased heat removal causes a shift in substrate concentration from a lower value to a higher value once the proportional control constant exceeds the threshold value (K_c). This suggests that the impact of heat removal on substrate concentration is different for different inhibition mechanisms. These findings underscore the significance of carefully considering temperature control and the specific characteristics of the inhibition system in order to optimize substrate concentration in the reactor.

Conclusions

This study focuses on the mathematical modelling and dynamical analysis of simple inhibition systems in enzyme-catalysed reactions within a CSTR. Three types of inhibition systems are considered: competitive, non-competitive, and uncompetitive. Bifurcation analyses are conducted to investigate the influence of varying system parameters. To demonstrate the parameter effects, the bifurcation diagrams of all three systems are presented in a single figure. The parameters under investigation are the dilution rate D , enzyme concentration ε , and proportional control constant K_c , which are adjusted accordingly.

Although all systems exhibit qualitatively similar behaviours, they have different threshold values. Increasing the dilution rate leads to a transition from low to high substrate concentrations, with three detected bifurcations, namely saddle node, Hopf and homoclinic bifurcation. The competitive inhibition system shows the highest bifurcation point due to the genuine competition between substrate and inhibitor. Conversely, increasing the enzyme concentration results in a decrease in substrate concentration because higher enzyme concentrations increase the availability of active sites. The non-competitive inhibition system has higher threshold values compared to other systems due to a decrease in the reaction's rate constant, requiring more enzymes to achieve the same conversion. The proportional control constant, which regulates heat removal, has varying effects depending on the system type. Consequently, caution must be exercised when attempting to control the reactor's heat.

Furthermore, codimension two bifurcation analysis is employed to examine the combined effects of dilution rate and proportional control on the systems, as depicted in the bifurcation diagrams. By utilizing this technique, the study reveals how the dilution rate, enzyme

concentration, and proportional control constant collectively determine the outcomes of this chemical system.

Recommendation for Future Research.

Based on the presented findings, several avenues for future research investigations are recommended:

- (i) **Experimental Validation:** It is advisable to conduct experimental studies to validate the mathematical models developed in this research. While experimental work in the context of finding of biocatalytic reactions and inhibition systems can be challenging, obtaining empirical data would serve as a crucial foundation for comparing and refining the mathematical models. This, in turn, would enhance the reliability and practical utility of these models.
- (ii) **Comparative Analysis with Different Reactor Configurations:** Given that the modelling work was conducted within the framework of a Continuous Stirred Tank Reactor (CSTR), it would be intriguing to expand the analysis to encompass other reactor configurations, such as a fed-batch reactor. A comparative examination of the system's dynamics and behaviours under diverse reactor conditions could yield valuable insights into the impact of reactor design on overall bioprocess performance.

Conflicts of Interest

The author(s) declare(s) that there is no conflict of interest regarding the publication of this paper.

Acknowledgment

The authors acknowledge support from the Fundamental Research Grant Scheme with Project Code: FRGS/1/2022/STG06/USM/02/1 by the Ministry of Higher Education, Malaysia (MOHE).

References

- [1] T. Palmer and P. L. Bonner. (2007). *Enzymes: Biochemistry, biotechnology, clinical chemistry*. Second Edition. Woodhead Publishing Limited.
- [2] F. P. Guengerich. (2017). *Mechanisms of enzyme catalysis and inhibition*. Third Edit. Elsevier.
- [3] R. L. Woosley, Y. Chen, J. P. Freiman, and R. A. Gillis. (1993). Mechanism of the Cardiotoxic Actions of Terfenadine. *JAMA J. Am. Med. Assoc.*, 269(12), 1532-1536.
- [4] C. H. Yun, R. A. Okerholm, and F. P. Guengerich. (1993). Oxidation of the antihistaminic drug terfenadine in human liver microsomes. Role of cytochrome P-450 3A(4) in N-dealkylation and C-hydroxylation, *Drug Metab. Dispos.*, 21(3), 403 LP-409.
- [5] J. F. Brady *et al.* (1991). Modulation of rat hepatic microsomal monooxygenase enzymes and cytotoxicity by diallyl sulfide. *Toxicol. Appl. Pharmacol.*, 108(2), 342-354.
- [6] U. Sharma, E. S. Roberts, and P. F. Hollenberg. (1996). Formation of a metabolic intermediate complex of cytochrome P4502B1 by clorgyline. *Drug Metab. Dispos.*, 24(11), 1247 LP-1253.
- [7] J. P. Van Wauwe and P. A. J. Janssen. (1989). Is there a case for P-450 inhibitors in cancer treatment? *J. Med. Chem.*, 32(10), 2231-2239.
- [8] H. Vanden Bossche. (1992). Inhibitors of P450-dependent steroid biosynthesis: From research to medical treatment. *J. Steroid Biochem. Mol. Biol.*, 43(8), 1003-1021.
- [9] I. H. Segel. (1975). *Enzyme kinetics: behavior and analysis of rapid equilibrium and steady state enzyme systems*. New York: Wiley.
- [10] R. S. Ochs. (2018). Understanding enzyme inhibition. *J. Chem. Educ.*, 77(11), 1453-1456.
- [11] N. S. Punekar. (2018). *Enzymes: Catalysis, kinetics and mechanisms*. Springer.
- [12] P. K. Robinson. (2015). Enzymes: Principles and biotechnological applications. *Essays Biochem.*, 59,1-41.
- [13] C. G. Whiteley. (2000). Enzyme kinetics: Partial and complete uncompetitive inhibition. *Biochem. Educ.*, 28(3), 144-147.
- [14] V. Q. Mai and T. A. Nhan. (2021). Numerical analysis of coupled systems of ODEs and applications to enzymatic competitive inhibition by product. *Adv. Theory Nonlinear Anal. its Appl.*, 5(1), 58-71.
- [15] A. Akgül, S. H. A. Khoshnaw, and A. S. Abdalrahman. (2020). Mathematical modeling for enzyme inhibitors with slow and fast subsystems. *Arab J. Basic Appl. Sci.*, 27(1), 442-449.
- [16] J. Mirón, M. P. González, J. A. Vázquez, L. Pastrana, and M. A. Murado. (2004). A mathematical model for glucose oxidase kinetics, including inhibitory, deactivant and diffusional effects, and their interactions. *Enzyme Microb. Technol.*, 34(5), 513-522.
- [17] G. L. Waldrop. (2009). A qualitative approach to enzyme inhibition. *Biochem. Mol. Biol. Educ.*, 37(1), 11-15.
- [18] M. Yoshino and K. Murakami. (2015). Analysis of the substrate inhibition of complete and partial types. *Springerplus*, 4(1).
- [19] M. Danish, M. Khaloofah, A. Mesfer, M. Rashid, and M. K. Al Mesfer. (2015). Effect of operating conditions

- on CSTR performance: An experimental study. *Int. J. Eng. Res. Appl.*, 5(2), 74-78.
- [20] C. Kravaris and I. K. Kookos. (2021). Understanding process dynamics and control. *Underst. Process Dyn. Control*.
- [21] A. Molnár, M. Krajčiová, J. Markoš, and L. Jelemenský. (2004). Use of bifurcation analysis for identification of a safe CSTR operability. *J. Loss Prev. Process Ind.*, 17(6), 489-498.
- [22] C. Van Heerden. (1953). Autothermic processes. *Ind. Eng. Chem.*, 45(6), 1242-1247.
- [23] A. S. Bommarius and B. R. Riebel. (2004). *Biocatalysis, Fundamentals and Applications*. John Wiley & Sons.
- [24] P. F. Hollenberg. (2022). Enzyme inhibition. *Drug Metabolism Handbook*, 407-425.
- [25] R. Aris and N. R. Amundson. (1958). An analysis of chemical reactor stability and control—II: The evolution of proportional control. *Chem. Eng. Sci.*, 7(3), 132-147.
- [26] M. R. M. Radzi and M. H. Uzir. (2009). Stability study of an exothermic biocatalytic reaction and its application in bioprocess systems, 17(June 2007), 95-115.
- [27] A. Uppal, W. H. Ray, and A. B. Poore. (1974). On the dynamic behavior of continuous stirred tank reactors. *Chem. Eng. Sci.*, 29(4), 967-985.
- [28] M. K. Purkait and D. Haldar. (2021). Strategies to improve enzymatic production of sugars. *Lignocellul. Biomass to Value-Added Prod.*, 95-109.
- [29] R. Aris and N. R. Amundson. (1958). An analysis of chemical reactor stability and control—I: The possibility of local control, with perfect or imperfect control mechanisms. *Chem. Eng. Sci.*, 7(3), 121-131.
- [30] Seborg. (2019). *Process dynamics and control*. Fourth Edition. Wiley.
- [31] M. Danish, M. K. Al Mesfer, and M. Rashid. (2015). Effect of operating conditions on CSTR performance: An experimental study. *J. Eng. Res. Appl.*, 5(2), 74-78.
- [32] N. Miložič, M. Lubej, M. Lakner, P. Žnidaršič-Plazl, and I. Plazl. (2017). Theoretical and experimental study of enzyme kinetics in a microreactor system with surface-immobilized biocatalyst. *Chem. Eng. J.*, 313, 374-381.
- [33] A. Matin, A. Grootjans, and H. Hogenhuis. (1976). Influence of dilution rate on enzymes of intermediary metabolism in two freshwater bacteria grown in continuous culture. *J. Gen. Microbiol.*, 94(2), 323-332.
- [34] C. Zhang and X. H. Xing. (2011). *Enzyme Bioreactors*. Second Edi. Elsevier.
- [35] R. Konnur and S. Pushpavanam. (1994). The dynamics of a fed-batch reactor: The transition from the batch to the CSTR. *Chem. Eng. Sci.*, 49(3), 383-392.
- [36] J. W. Swarts, R. C. Kolfschoten, M. C. A. A. Jansen, A. E. M. Janssen, and R. M. Boom. (2010). Effect of diffusion on enzyme activity in a microreactor. *Chem. Eng. J.*, 162(1), 301-306.
- [37] A. Uppal, W. H. Ray, and A. B. Poore. (1976). The classification of the dynamic behavior of continuous stirred tank reactors-influence of reactor residence time. *Chem. Eng. Sci.*, 31(3), 205-214.
- [38] D. Paolucci-Jeanjean, M. P. Belleville, G. M. Rios, and N. Zakhia. (2000). The effect of enzyme concentration and space time on the performance of a continuous recycle membrane reactor for one-step starch hydrolysis. *Biochem. Eng. J.*, 5(1), 17-22.
- [39] R. Ball and B. F. Gray. (2013). Thermal instability and runaway criteria: The dangers of disregarding dynamics. *Process Saf. Environ. Prot.*, 91(3), 221-226.
- [40] R. Ball and B. F. Gray. (1999). Thermal stabilization of chemical reactors II. Bifurcation analysis of the Endex CSTR. *Proc. R. Soc. A Math. Phys. Eng. Sci.*, 455(1992), 4223-4243.
- [41] R. M. Daniel, M. J. Danson, R. Eisenthal, C. K. Lee, and M. E. Peterson. (2008). The effect of temperature on enzyme activity: New insights and their implications. *Extremophiles*, 12(1), 51-59.
- [42] K. T. Lu, K. M. Luo, T. F. Yeh, and P. C. Lin. (2008). The kinetic parameters and safe operating conditions of nitroglycerine manufacture in the CSTR of Biazzi process. *Process Saf. Environ. Prot.*, 86(1B), 37-47.